JACC: BASIC TO TRANSLATIONAL SCIENCE
PUBLISHED BY ELSEVIER ON BEHALF OF THE AMERICAN COLLEGE OF CARDIOLOGY FOUNDATION. THIS IS AN OPEN ACCESS ARTICLE UNDER THE CC BY-NC-ND LICENSE (http://creativecommons.org/licenses/by-nc-nd/4.0/).

VOL. 7, NO. 12, 2022

ORIGINAL RESEARCH - PRECLINICAL

Targeting the Autophagy-Lysosome Pathway in a Pathophysiologically Relevant Murine Model of Reversible Heart Failure

Sarah Evans, PhD,[a] Xiucui Ma, PHD,[a] Xiqiang Wang, MD,[a] Yana Chen, PHD,[b] Chen Zhao, BS,[a] Carla J. Weinheimer, MS,[a] Attila Kovacs, MD,[a] Brian Finck, PhD,[a,b] Abhinav Diwan, MD,[a] Douglas L. Mann, MD[a]

VISUAL ABSTRACT

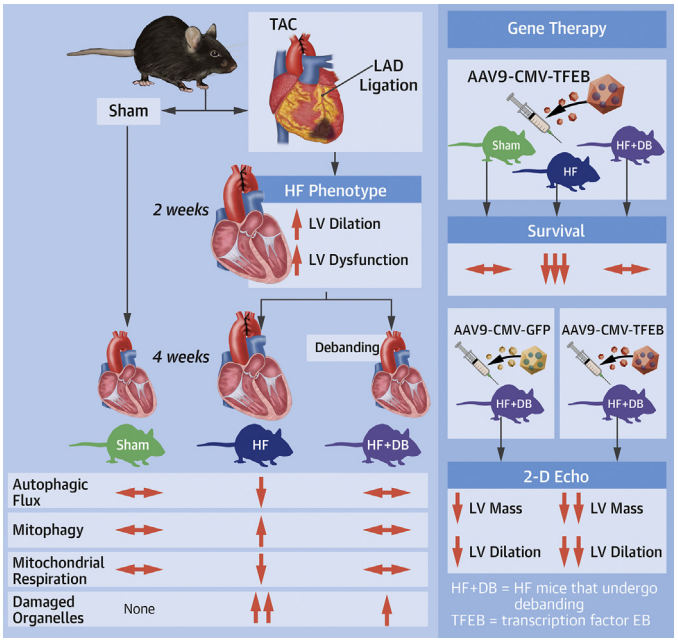

Evans S, et al. J Am Coll Cardiol Basic Trans Science. 2022;7(12):1214–1228.

HIGHLIGHTS

- The biological drivers of reverse LV remodeling are not well understood.
- Transaortic constriction induced hemodynamic pressure overload superimposed on acute LAD ligation in mice resulted in increased mammalian target of rapamycin activation, decreased autophagic flux, increased mitophagy, decreased mitochondrial oxidative capacity, and accumulation of damaged proteins and organelles in cardiac myocytes
- Hemodynamic unloading by removing the transaortic constriction leads to reverse LV remodeling, increased mammalian target of rapamycin activation, restoration of autophagic flux, and normalization of mitochondrial oxidative capacity, but incomplete removal of damaged proteins and organelles
- Enhancing autophagic flux with AAV9- CMV-transcription factor EB in mice that have undergone hemodynamic unloading resulted in more favorable reverse LV remodeling compared with control mice treated with AAV9-CMV-GFP, whereas treating mice that have not undergone hemodynamic unloading with AAV9-CMV-transcription factor EB leads to increased lethality.

From the [a]Center for Cardiovascular Research, Cardiovascular Division, Washington University School of Medicine, St. Louis, Missouri, USA; and the [b]Division of Geriatrics & Nutritional Science, Washington University School of Medicine, St. Louis, Missouri, USA.

Junichi Sadoshima MD, PhD, served as Guest Associate Editor for this paper. Michael Bristow, MD, PhD, served as the Guest Editor-in-Chief for this paper.

ISSN 2452-302X https://doi.org/10.1016/j.jacbts.2022.06.003

SUMMARY

The key biological "drivers" that are responsible for reverse left ventricle (LV) remodeling are not well understood. To gain an understanding of the role of the autophagy-lysosome pathway in reverse LV remodeling, we used a pathophysiologically relevant murine model of reversible heart failure, wherein pressure overload by transaortic constriction superimposed on acute coronary artery (myocardial infarction) ligation leads to a heart failure phenotype that is reversible by hemodynamic unloading. Here we show transaortic constriction + myocardial infarction leads to decreased flux through the autophagy-lysosome pathway with the accumulation of damaged proteins and organelles in cardiac myocytes, whereas hemodynamic unloading is associated with restoration of autophagic flux to normal levels with incomplete removal of damaged proteins and organelles in myocytes and reverse LV remodeling, suggesting that restoration of flux is insufficient to completely restore myocardial proteostasis. Enhancing autophagic flux with adeno-associated virus 9-transcription factor EB resulted in more favorable reverse LV remodeling in mice that had undergone hemodynamic unloading, whereas overexpressing transcription factor EB in mice that have not undergone hemodynamic unloading leads to increased mortality, suggesting that the therapeutic outcomes of enhancing autophagic flux will depend on the conditions in which flux is being studied. (J Am Coll Cardiol Basic Trans Science 2022;7:1214–1228) Published by Elsevier on behalf of the American College of Cardiology Foundation. This is an open access article under the CC BY-NC-ND license (http://creativecommons.org/licenses/by-nc-nd/4.0/).

ABBREVIATIONS AND ACRONYMS

AAV9 = adeno-associated virus 9

CMV = cytomegalovirus

CQ = chloroquine

dsDNA = double stranded DNA

eGFP = enhanced green fluorescent protein

GFP = green red fluorescent protein

HF = heart failure

HF-DB = TAC + MI mice that have undergone debanding

LV = left ventricle

LFEF = left ventricular ejection fraction

MI = myocardial infarction

mTOR = mammalian target of rapamycin

RFP = red fluorescent protein

TAC = transaortic constriction

TEM = transmission electron microscopic

TFEB = transcription factor EB

Medical and device therapies that reduce morbidity and mortality in patients with heart failure (HF) with a reduced left ventricular (LV) ejection fraction also lead to decreased LV volume and mass, and a more normal elliptical shape of the ventricle, resulting in a leftward shift of the end-diastolic pressure volume relationship toward normal values, which has been referred to as reverse LV remodeling.[1,2] Although a number of cellular, molecular, and anatomic changes that occur during reverse LV remodeling have been identified, the key biological "drivers" that are responsible for reverse LV remodeling are not at all well understood (reviewed in references[3,4]).

Several biological themes have emerged with respect to our understanding of reverse LV remodeling. First, reverse LV remodeling occurs after removal of the inciting stress that led to forward LV remodeling (eg, hemodynamic overload, neurohormonal stress). Second, many of the cellular and anatomic changes that occur during forward LV remodeling revert toward the normal less pathologic phenotype during reverse LV remodeling.[4,5] Third, a significant proportion of the multilevel molecular changes that occur during forward LV remodeling remain persistently dysregulated in reverse remodeled hearts, despite improvements in structural and functional abnormalities. Thus, reverse LV remodeling is not simply a mirror image of forward LV remodeling, but represents a transition to a new less pathologic condition that allows the heart to maintain preserved pumping capacity.

Transcriptional profiling of reverse remodeled hearts also revealed the emergence of new sets of genes that belong to ontogenies that are not expressed in nonfailing hearts,[5] including gene ontogenies involved in tissue repair.[6,7] Recognizing that genes involved in protein quality control are upregulated in experimental models of reversible HF, and recognizing that the autophagy-lysosome system serves as a dynamic recycling system that provides new building blocks for cellular renovation and homeostasis of cells,[8] we sought to determine the role of the autophagy-lysosome pathway in a pathophysiologically relevant murine model of HF[7] wherein hemodynamic unloading leads to reversal of the HF phenotype. Here, we show that pressure overload superimposed on acute coronary artery ligation leads to decreased flux through the autophagy-lysosome pathway with the accumulation of damaged proteins and organelles in cardiac myocytes, whereas hemodynamic unloading is associated with restoration of autophagic flux to normal levels with incomplete removal of damaged proteins and organelles in myocytes and reverse LV remodeling, suggesting that restoration of flux is insufficient to completely restore

The authors attest they are in compliance with human studies committees and animal welfare regulations of the authors' institutions and Food and Drug Administration guidelines, including patient consent where appropriate. For more information, visit the Author Center.

Manuscript received April 7, 2022; revised manuscript received June 1, 2022, accepted June 1, 2022.

myocardial proteostasis. The failure to effectively restore essential cytosolic components in cardiac myocytes may lead to a loss of cellular resilience[9] or loss of contractile reserve, which in turn may provide insights into the biological basis for why HF recurs (ie, relapse) in patients who have been treated with evidence-based medical and/or device therapies.

METHODS

PATHOPHYSIOLOGICALLY RELEVANT MURINE MODEL OF REVERSIBLE HF. We developed a pathophysiologically relevant reversible mouse model of HF that combines moderate transaortic constriction (TAC) and distal LAD ligation (myocardial infarction [MI]) that leads to pathophysiological LV remodeling greater than is observed with either TAC or MI alone.[7] Specifically TAC + MI mice develop progressive LV dilation and LV dysfunction and a HF phenotype 2-6 weeks after TAC + MI.[7] The HF phenotype can be reversed by debanding the aorta 2 weeks after TAC + MI. The hemodynamic unloading after debanding leads to normalization of LV volumes, normalization of LV mass, normalization of cardiac myocyte hypertrophy, and reversal of the HF phenotype.[7]

For the purposes of the studies described herein, we studied 3 groups of female C57BL/6 mice (Jackson Laboratory) that were subjected to TAC + MI at 8 weeks of age: 1) mice subjected to combined TAC + MI (referred to as HF mice) followed for 6 weeks; 2) HF mice subjected to aortic debanding at 2 weeks post-TAC + MI and followed for 4 weeks after debanding (referred to as HF-DB mice); and 3) sham mice subjected to the identical procedures, except for the tightening of the coronary artery and aortic ligatures, followed for 6 weeks (referred to as sham mice) (see Supplemental Figure 1 for experimental protocol).

All experiments were performed according to the recommendations of the Guide for the Care and Use of Laboratory Animals, 8th Edition (National Research Council. *Guide for the Care and Use of Laboratory Animals: Eighth Edition*. Washington, DC: The National Academies Press, 2011) and were approved by the Animal Care and Use Committee at Washington University.

CHARACTERIZATION OF AUTOPHAGIC FLUX. Autophagic flux was assessed in the sham, HF, and HF-DB mice at 6 weeks after TAC-MI by injecting the mice with chloroquine (CQ), 40 mg/kg intraperitoneal, 4 hours before humane killing, and then examining the accumulation of LC3-II and p62 using Western blotting of cardiac extracts, as an indicator of flux through the macro-autophagy pathway.[10] As a second measure of autophagy, we determined autophagosome and lysosome abundance at 6 weeks after TAC+ MI in sham, HF, and HF-DB mice using immunofluorescence examination of frozen myocardial tissue from *CAG-RFP-EGFP-LC3* reporter mice that express the autophagosome protein LC3 fused in tandem to both red fluorescent protein (RFP) and enhanced green fluorescent protein (EGFP). Combined green fluorescent protein (GFP) and RFP fluorescence within autophagosomes, which have a physiological pH, emit a yellow fluorescent signal, whereas the EGFP signal is quenched in the acidic environment of autolysosomes, which only emit a RFP signal, as described.[11] The *CAG-RFP-EGFP-LC3* mice were purchased from Jackson Laboratory (strain 027139) and were bred in-house.

IMMUNOBLOTTING. Crude cardiac extracts of the sham, HF, and HF-DB hearts were prepared at 6 weeks, followed by immunoblotting, as described.[12] For studies involving subcellular fractionation into cytoplasmic and nuclear fractions, hearts were fractionated into nucleus-enriched and cytoplasmic samples using a CelLytic NuCLEAR extraction kit (Sigma), as described.[13] The antibodies used were as follows: Lysosomal Associated Membrane Protein 2 (LAMP2), mouse monoclonal (Developmental Studies Hybridoma Bank, ABL-93); LAMP1 (Santa Cruz Biotechnology, sc-19992); anti-LC3 (encoding for Microtubule Associated Protein 1 Light Chain 3 Beta [MAP1LC3B]) subunit, Novus Biologicals, NB100-2220; Sequestosome 1 (SQSTM1, p62, Abcam, ab5416); transcription factor EB (TFEB, Bethyl Labs, A303-673A); p70S6K (phosphorylated ribosomal protein S6 kinase beta-1, 2708, Cell Signaling); phosphorylated p70S6K (9234, Cell Signaling); eukaryotic translation initiation factor 4E-binding protein 1 (4EBP1, 9644, Cell Signaling); phosphorylated 4EBP1 (2855, Cell Signaling); phosphorylated mammalian target of rapamycin (mTOR) (2974, Cell Signaling); mTOR (2983, Cell Signaling); histone H3 (9715, Cell Signaling); glyceraldehyde-3-phosphate dehydrogenase (GAPDH) (ab22555, Abcam); actin (Sigma, A2066); Cathepsin D (a gift from Stuart Kornfeld, Washington University, St. Louis, Missouri, USA); Ubiquitin (ab179434, Abcam); cytochrome C oxidase-IV (COX-IV, Abcam, ab14744); and translocase of the outer mitochondrial membrane 20 (Tomm20, Sigma, MFCD04118702).

TRANSMISSION ELECTRON MICROSCOPY. For ultrastructural analyses, tissue samples were fixed in 2% paraformaldehyde/2.5% glutaraldehyde (Ted Pella Inc) in 100 mmol/L sodium cacodylate buffer for 2 hours at room temperature and then overnight at 4°C. Samples were washed in sodium cacodylate buffer

and postfixed in 2% osmium tetroxide (Ted Pella Inc) for 1 hour at room temperature. After 3 washes in dH_2O, samples were en bloc stained in 1% aqueous uranyl acetate (Electron Microscopy Sciences) for 1 hour. Samples were then rinsed in dH_20, dehydrated in a graded series of ethanol, and embedded in Eponate 12 resin (Ted Pella Inc). Sections of 95 nm were cut with a Leica Ultracut UCT ultramicrotome (Leica Microsystems Inc), stained with uranyl acetate and lead citrate, and viewed on a JEOL 1200 EX transmission electron microscope (JEOL USA Inc) equipped with an AMT 8 megapixel digital camera and AMT Image Capture Engine V602 software (Advanced Microscopy Techniques). Processing and imaging was performed at the Molecular Microbiology Imaging Facility at Washington University School of Medicine.

MITOCHONDRIAL RESPIRATION. High-resolution respirometry was performed as previously described.[14] All studies were performed in the sham, HF, and HF-DB mice 4 weeks after TAC + MI or sham surgery. A section of the LV lateral wall was freshly excised, the fibers were separated, permeabilized, washed, blotted dry, and then weighed. One to 2 mg of tissue were placed in an Oxygraph 2K (OROBOROS Instruments) chamber containing 2 mL of MirO5 with 20 mmol/L creatinine monohydrate and 10 μmol/L blebbistatin. To measure O_2 flux, the following substrates were added sequentially and measurements were performed at steady state with DatLab Software (OROBOROS Instruments; final concentrations indicated): 1) leak: 0.5 mmol/L malate, 5 mmol/L pyruvate, 10 mmol/L glutamate; 2) complex I: 5 mmol/L adenosine diphosphate; 3) complex I + II: 10 mmol/L succinate; and 4) complex II: 0.5 μmol/L rotenone. All measures were normalized to tissue weight.

ASSESSMENT OF MITOPHAGY. Mitophagy was assessed by determining the colocalization of PicoGreen (a fluorescent sensor specific for double stranded DNA [dsDNA]) with LC3 in the hearts of sham, HF, and HF-DB mice. Briefly, at 6 weeks mice were humanely killed, the hearts were removed and weighed, and the midpapillary sections were fixed in 10% formalin and paraffin-embedded. Paraffin sections were immunostained with an anti-LC3 antibody, PicoGreen (Quant-iT PicoGreen dsDNA Assay Kit, Thermo Fisher Scientific, P7589), and an Alexa Fluor 594 donkey anti-rabbit secondary antibody as described.[15] Colocalization of dsDNA with LC3 results in a yellow fluorescent signal that is indicative of mitophagy.[16] Confocal imaging was performed on a Zeiss confocal LSM-700 laser scanning confocal microscope using 639 Zeiss Plan-Neofluar 40/1.3 and 63/1.4 oil immersion objectives, and images were acquired using Zen 2010 software. Mitochondrial abundance evaluating the relative abundance of COX-IV and TOMM20 using Western blotting.

GENERATION OF ADENO-ASSOCIATED VIRUS CONSTRUCTS. Mouse TFEB complementary DNA (or GFP as a control) was cloned into an adeno-associated virus (AAV) vector containing the cytomegalovirus (CMV) promoter (pAAV-CMV-TFEB), as previously described.[13] A pAAV-CMV-GFP construct was used as the appropriate control AAV9 particles were generated at the Hope Center Viral Vectors Core at Washington University School of Medicine. A 1-time dose of 3.5×10^{11} particles was administered to the HF mice by tail vein injection 2 weeks after sham surgery or TAC + MI and to the HF-DB mice 2 weeks after sham surgery or TAC + MI after debanding.

ECHOCARDIOGRAPHIC STUDIES. Image acquisition. Ultrasound examination of the cardiovascular system was performed using a Vevo 2100 Ultrasound System (VisualSonics Inc) equipped with a 30-MHz linear-array transducer, as previously described.[7]

Imaging protocol. The HF-DB mice were imaged using 2-dimensional echocardiography 2 weeks after TAC + MI and before debanding. The mice were then debanded and treated with AAV9-CMV-TFEB and AAV9-CMV-GFP and imaged again 4 weeks later to evaluate the effects of TFEB transduction on LV remodeling (Supplemental Figure 1B).

STATISTICAL ANALYSIS. Data are presented as the mean ± SEM. All measurements were obtained on distinct biological replicates. Statistics were performed in Prism Version 8.0.2 (GraphPad Software). Data were tested for assumptions of normality with the Shapiro-Wilk normality test. If the samples were normally distributed a parametric statistical analysis was performed using unpaired 2-tailed Student's *t*-test for 2 group comparisons, or 1-way analysis of variance to determine mean differences between multiple groups; where appropriate, post hoc testing with Dunnett or Tukey test for multiple pairwise comparisons was used. If the samples were not normally distributed, we performed Kruskal-Wallis testing for multiple group analysis with Dunn post hoc testing or Mann-Whitney testing for 2 groups. For Kaplan-Meier analysis of survival curves, the log-rank test was used. A P value <0.05 was considered statistically significant.

RESULTS

CHARACTERIZATION OF AUTOPHAGIC FLUX IN A MODEL OF REVERSIBLE HF. To examine the state of activation of myocardial autophagy during TAC stress

and with debanding, we assessed autophagic flux in the HF and HF-DB mice. In the context of the present discussion, the autophagic flux refers to autophagosome formation, sequestration of cargo in the autophagosome, delivery of the cargo to a lysosome, and degradation of the cargo in the lysosome.[17] Autophagic flux was assessed in sham, HF, and HF-DB mice at 6 weeks by injecting the mice with CQ (40 mg/kg) or diluent intraperitoneally 4 hours before humane killing, and then examining the accumulation of LC3-II and p62 in cardiac extracts as an indicator of flux through the macro-autophagy pathway.[10] As shown in the representative Western blots in **Figure 1A**, and the group data in **Figures 1B and 1C**, short-term treatment with CQ resulted in an expected accumulation of LC3-II (a marker of autophagosome abundance) ($P = 0.044$) and p62 (a reporter of autophagic flux) ($P = 0.002$) in the sham mice, reflecting intact autophagic flux. In contrast, there was no significant change in the levels of autophagosome-bound LC3-II ($P = 0.96$) or p62 ($P = 0.058$) in the CQ-treated HF mice when compared with the respective diluent-treated HF mice (**Figures 1A to 1C**), suggesting that there was reduced autophagosome turnover and impaired flux in the HF mice. Examination of autophagic flux in HF-DB mice (**Figures 1A to 1C**) demonstrated a return to a state of preserved flux with significant increases in LC3-II ($P = 0.029$) and p62 ($P = 0.016$) levels in CQ-treated vs respective diluent-treated HF-DB animals, at levels comparable with those observed in the sham group.

As a second measure of autophagic flux, we determined autophagosome and autolysosome abundance in myocardial sections in sham, HF, and HF-DB using a *CAG-RFP-EGFP-LC3* transgenic reporter mouse,[18] in which the CAG promoter/enhancer sequences drive the expression of a RFP, EGFP, and LC3 (to tag the reporter construct to autophagosomes and lysosomes). Combined GFP and RFP fluorescence within autophagosomes, which are at physiological pH, yields a yellow signal, whereas EGFP is quenched in the acidic environment of autolysosomes, which only emit a RFP signal. Given that autophagosomes turnover via fusion with lysosomes to form autolysosomes, the relative abundance of autolysosomes to autophagosomes is a readout of autophagic flux. **Figures 1D and 1E** show that autophagosome abundance was not different among the sham, HF, and HF-DB mice at 6 weeks ($P = 0.33$ by analysis of variance), whereas there was a significant decrease ($P = 0.026$) in the RFP signal in the HF mice (relative to sham), indicating a reduced abundance of autolysosomes. Hemodynamic unloading in the HF-DB mice restored the RFP signal relative to sham levels ($P = 0.81$), indicating an increase in autolysosome abundance. Viewed together, these findings suggest that there is impaired autophagic flux with reduced autophagosome turnover in the HF mice, and that hemodynamic unloading of the HF mice restores autophagic flux.

IMPAIRED AUTOPHAGIC FLUX IS ASSOCIATED WITH ACCUMULATION OF POLYUBIQUITINATED PROTEINS AND DAMAGED ORGANELLES IN A MODEL OF REVERSIBLE HF.

To determine whether impaired autophagic flux in the HF mice resulted in the accumulation of damaged proteins and/or organelles, we measured the abundance of Lys 63 polyubiquitinated substrates, the primary ubiquitin chain type for autophagic targeting,[19] and we examined transmission electron microscopic (TEM) images of cardiac myocytes in the sham, HF, and HF-DB mice. As shown in the representative Western blot in **Figure 2A** and the group data in **Figure 2B**, there was a significant increase in Lys 63 polyubiquitinated substrates in the HF ($P = 0.018$) and HF-DB mice ($P = 0.009$) when compared with the sham controls. Importantly, the accumulation of Lys 63 polyubiquitinated substrates was not significantly different ($P = 0.94$) between the HF and the HF-DB mice. TEM imaging of sham, HF, and HF-DB mouse hearts (**Figure 2C**) showed that there was an increase in abundance of double membrane-bound autophagosomes (white arrows), accumulation of small round mitochondria, and rarefaction of mitochondrial cristae (black arrows), as well as evidence for swollen endoplasmic reticulum (white arrowheads) in the HF and HF-DB mouse hearts. The aspect ratio (length/width ratio) of mitochondria serves as a proxy for assessing the extent to which mitochondria are networked (a higher aspect ratio indicates more highly fused tubular mitochondria). Analysis of the mitochondrial aspect ratio in the sham, HF, and HF-DB mice revealed that there was a significant ($P = 0.009$) decrease in mitochondrial aspect ratio in the HF mice compared with sham, indicating a transition from elongated morphology to more rounded mitochondria, consistent with mitochondrial fission (**Figure 2D**). Although the mitochondrial aspect ratio increased numerically in the hearts of the HF-DB mice, the change in the aspect ratio was not significantly different ($P = 0.14$) from sham values. There was no significant difference in the relative abundance of COX-IV ($P = 0.89$) and TOMM20 ($P = 0.24$) protein levels in the hearts of the sham, HF, and HF-DB mice (Supplemental Figure 2), indicating that mitochondrial abundance was maintained in the HF and HF-DB mice. Viewed together, these data demonstrate that there is an accumulation of Lys 63 polyubiquitinated proteins and damaged organelles in the hearts of the HF mice with impaired autophagic flux, and that the

FIGURE 1 Autophagic Flux in a Model of Reversible HF

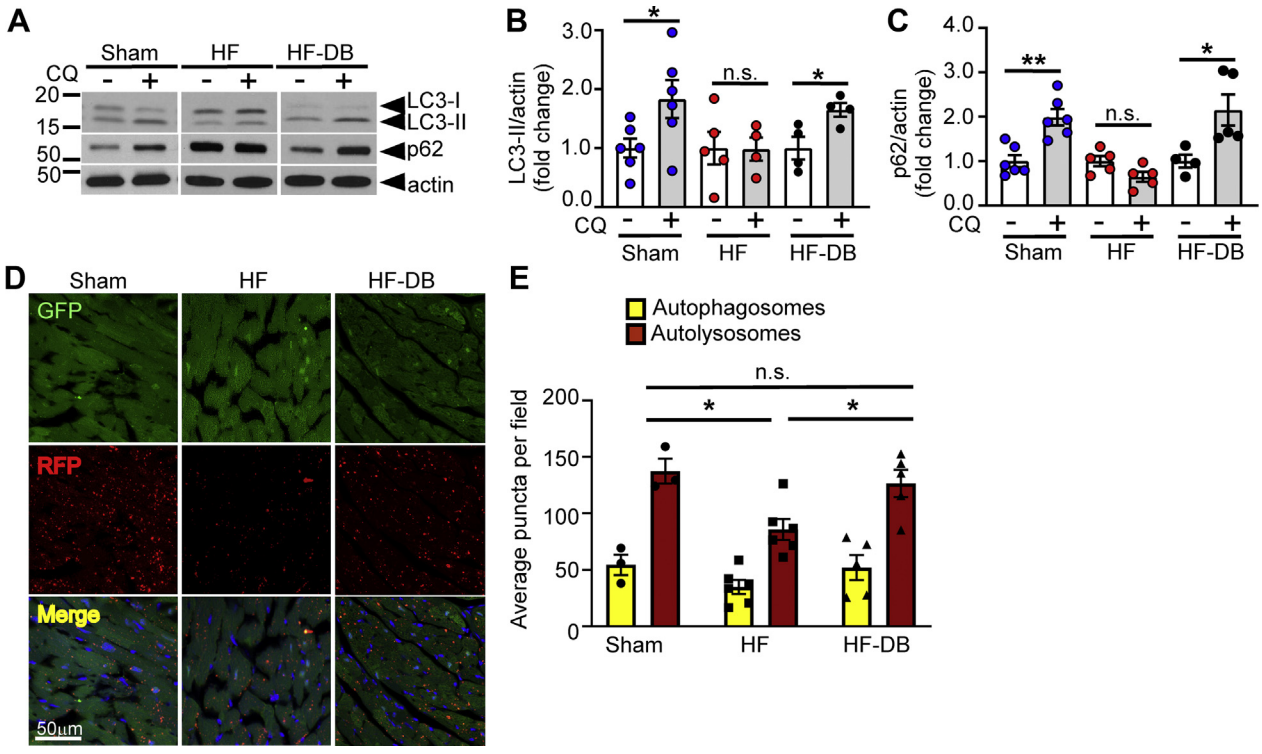

Autophagic flux was determined in sham, heart failure (HF), and heart failure-deband (HF-DB) mice at 6 weeks by measuring the accumulation of LC3-II and p62 proteins in cardiac extracts (see Methods and Supplemental Figure 1A). **(A)** Representative immunoblots of LC3-II and p62 levels with (+) and without (-) chloroquine pre-treatment. Each pair of + and – chloroquine samples was run on adjacent lanes on the same gel and blotted for LC3-II, p62, and actin. Sham, HF, and HF-DB pairs were cut From separate blots and combined for the representative images. **(B)** Group data for LC3-II levels relative to actin loading controls (n = 4-6 mice/group) (*t* test) and **(C)** group data for p62 levels relative to actin loading controls (n = 4-6 mice/group) (*t* test for sham and HF) (Mann-Whitney test for HF-DB). Autophagosome and autolysosome abundance was determined using immunofluorescence microscopy of myocardial sections from sham, HF, and HF-DB *CAG-RFP-EGFP-LC3* reporter mice at 6 weeks. **(D)** Representative fluorescent micrographs (scale bar = 50 μm). **(E)** Group data for abundance of autolysosomes (**red** fluorescent puncta) and autophagosomes (**yellow** fluorescent puncta) per 40X field (n = 3-6 mice/group) (Tukey test). *$P < 0.05$, **$P < 0.01$. n.s. = nonsignificant.

accumulation of damaged proteins and organelles persists in the hearts of the HF-DB mice after hemodynamic unloading and normalization of autophagic flux. These findings suggest that the restoration of flux in the HF-DB mouse hearts is not sufficient to restore cardiac myocyte protein homeostasis (proteostasis) and organelle quality.

MECHANISM OF IMPAIRED AUTOPHAGIC FLUX IN A MODEL OF REVERSIBLE HF. To explore the mechanism(s) for the impaired autophagic flux in the HF mice, we measured protein levels of LAMP1, LAMP2, and pro-cathepsin, which reflect the abundance of lysosomal proteins, as well as mTOR activation, which is known to regulate multiple steps of the autophagy process after hemodynamic unloading. Figure 3 shows that there was a significant increase in LAMP1 ($P = 0.010$) and pro-cathepsin ($P = 0.012$) and a numeric increase in LAMP2 ($P = 0.082$) protein levels in the HF mice relative to sham control mice (Figure 1E). Hemodynamic unloading of the HF-DB mice resulted in a decrease in LAMP1, LAMP2, and pro-cathepsin levels to values observed in sham-operated control mice (Figures 3C and 3D). Notably, there was a significant ($P = 0.048$) increase in mTOR activation, denoted by increased mTOR phosphorylation, whereas there was a numeric increase in the phosphorylation of substrates of mTOR signaling, namely, p70S6 Kinase ($P = 0.15$) and a 4EBP1 ($P = 0.092$) in the HF mice when compared with sham-operated mice. Hemodynamic unloading of the HF-DB led to normalization of mTOR, p70S6 Kinase, and 4EBP1 phosphorylation levels to those observed in sham controls (Figures 3E to 3G). Viewed together, these observations suggest a potentially important role for mTOR with respect to modulating autophagic flux in the HF and HF-DB mice.

FIGURE 2 Accumulation of Polyubiquitinated Proteins and Damaged Organelles in a Model of Reversible HF

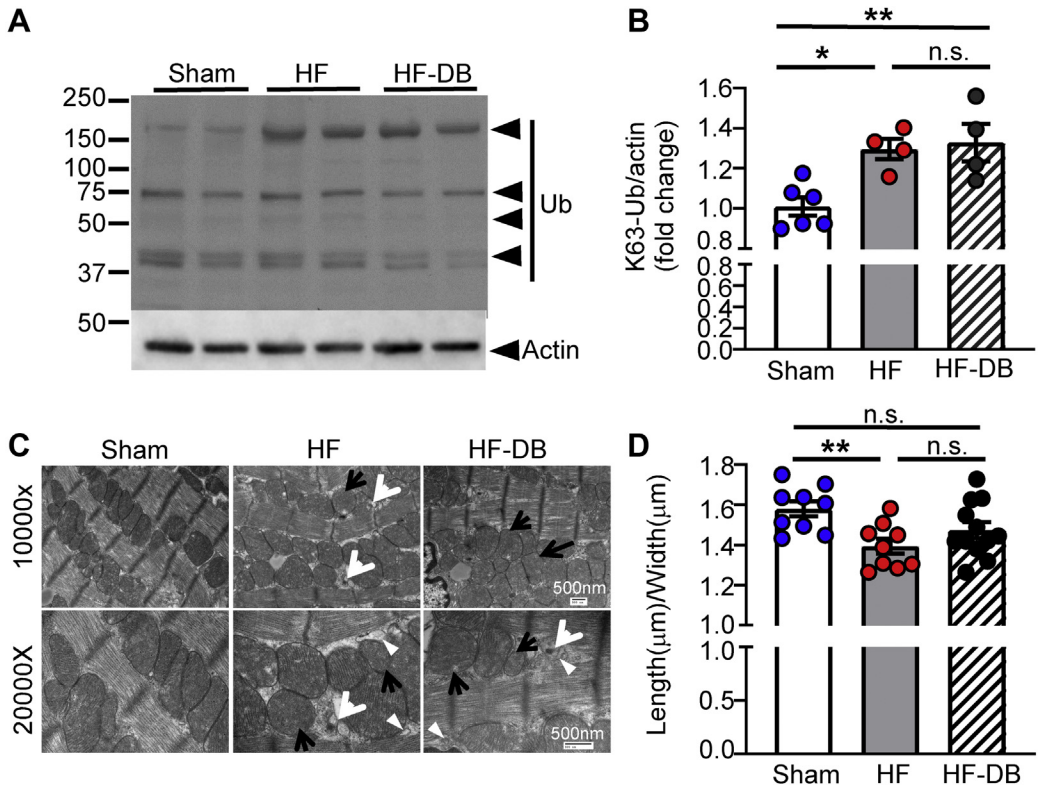

(A) Representative immunoblots depicting levels of Lys63 polyubiquitinated proteins in sham, HF, or HF-DB mice at 6 weeks. **(B)** Group data for Lys63 polyubiquitinated proteins relative to actin loading control in sham, HF, or HF-DB mice (n = 4-6 mice/group) (Tukey test). **(C)** Representative transmission electron microscopy (TEM) images of cardiac tissue from sham, HF, or HF-DB mice at 6 weeks. Scale bar = 50 nm. **Large white arrows** depict double membrane-bound autophagosomes, **white arrowheads** denote endoplasmic reticulum, **black arrows** indicate mitochondria. **(D)** Group data for the mitochondrial aspect ratio (ratio of length/width) of sham, HF and HF-DB mice determined from TEM images (n = 9-12 images from 3-4 hearts/group) (Tukey test). *$P < 0.05$, **$P < 0.01$. Abbreviations as in Figure 1.

MITOCHONDRIAL RESPIRATION AND MITOPHAGY IN A MODEL OF REVERSIBLE HF. Given that our TEM imaging data suggested that there was an accumulation of damaged mitochondria in the hearts of HF and HF-DB mice (Figure 2C), we assessed mitochondrial oxidative capacity in sham, HF, and HD-DB mice using high-resolution respirometry (Oxygraph O2k, Oroboros Instruments), as described.[14] Figure 4 shows that maximal mitochondrial respiration mediated by complex I ($P < 0.001$ [measured by adding adenosine diphosphate]), complex I-II ($P < 0.001$ [measured by adding succinate]), and complex II ($P = 0.008$ [measured by subsequent addition of rotenone]) were significantly decreased in HF mice compared with sham, but that mitochondrial oxidative capacity returned to normal (sham) values in the HF-DB mice.

We also assessed mitophagic targeting of damaged mitochondria in the hearts of sham, HF, and HF-DB mice, by assessing the colocalization of dsDNA with LC3, as described.[20] Figure 4D depicts representative fluorescence micrographs, whereas the group data are illustrated in Figure 4E. There was increased colocalization of dsDNA with LC3 (denoted by yellow fluorescence [white arrowheads]) in the HF mice relative to the degree of colocalization in sham mice, consistent with a significant ($P < 0.001$) increase in mitochondria within autophagic structures in the HF mice. In contrast, the degree of colocalization of dsDNA with LC3 was not significantly different ($P = 1.00$) in the HF-DB mice from the sham operative control mice. Given that damaged mitochondria were detectable in hearts of the HF-DB mice (Figure 2D), these data suggest that mitophagy was insufficient to maintain mitochondrial protein quality control in the HF-DB mice.

FIGURE 3 Characterization of Autophagy-Related Proteins

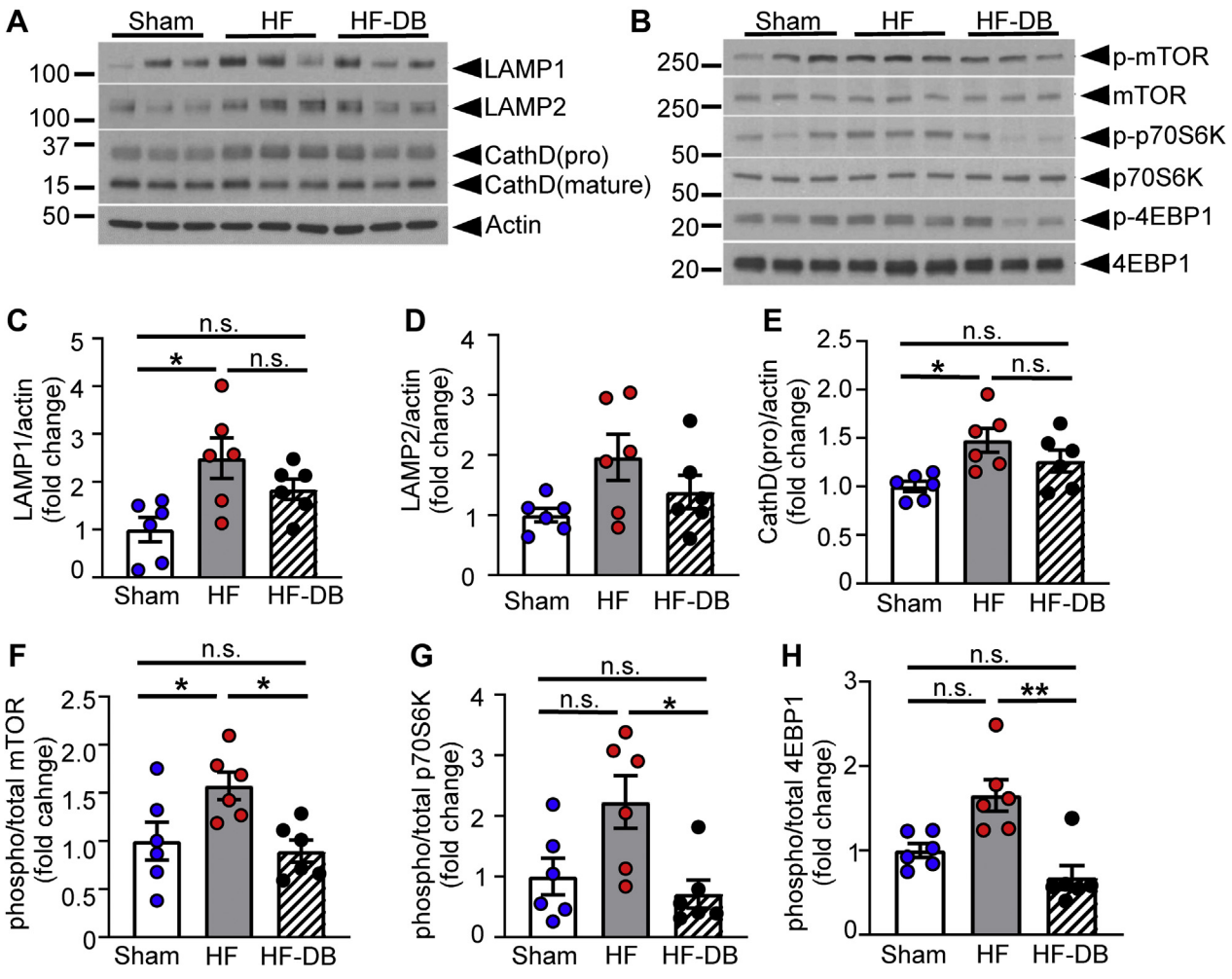

(A) Representative immunoblots of LAMP1, LAMP2, cathepsin D, and actin loading controls at 4 weeks. Samples derived from same experiment and blots processed in parallel. **(B)** Representative immunoblots of phospho-mTOR, total mTOR, phospho-p70s6K, total p70s6K, phospho-4EBP1, and total 4EBP1. Samples derived from same experiment and blots processed in parallel. Group data (n = 6 mice/group) for levels of **(C)** LAMP1 (Tukey test), **(D)** LAMP2 (Tukey test), **(E)** Cathepsin D (pro) (Tukey test) relative to actin loading controls. Group data (n = 6 mice/group) for the ratio of **(F)** phospho-mTOR to total mTOR (Tukey test); **(G)** phospho-p70s6K to total p70s6K (Dunn test), **(H)** phospho-4EBP1 to total 4EBP1 (Dunn test). *$P < 0.05$, **$P < 0.01$. mTOR = mammalian target of rapamycin; other abbreviations as in Figure 1.

MYOCARDIAL TFEB ACTIVATION IN A MODEL OF REVERSIBLE HF. Given the central role of TFEB as a master regulator of the autophagy-lysosome pathway,[21] we examined TFEB activation in the hearts of the HF and HF-DB hearts 6 weeks after TAC + MI. As shown in Supplemental Figure 3, there was a significant decrease in phosphorylated TFEB in the nucleus of HF mice compared with sham mice, consistent with inactivation of TFEB in the myocardium.[22] Although hemodynamic unloading resulted in an increase in nuclear TFEB levels in the HF-DB mice, consistent with TFEB activation (Supplemental Figure 3), the observation that polyubiquinated proteins and damaged organelles were present in the hearts of the HF-DB mice (Figure 2) suggested that autophagy-lysosome machinery was insufficient to restore cardiac myocyte proteostasis.

To determine whether TFEB-mediated enhancement would to lead to improved protein and quality control we treated the sham, HF, and HF-DB with AAV9-CMV-TFEB at the time of hemodynamic unloading of the HF-DB mice or sham surgery in the HF mice (Supplemental Figure 1). We have shown previously that this strategy results in a ~1.5- to 2-fold up-regulation of nuclear TFEB

FIGURE 4 Mitochondrial Respiration and Mitophagy

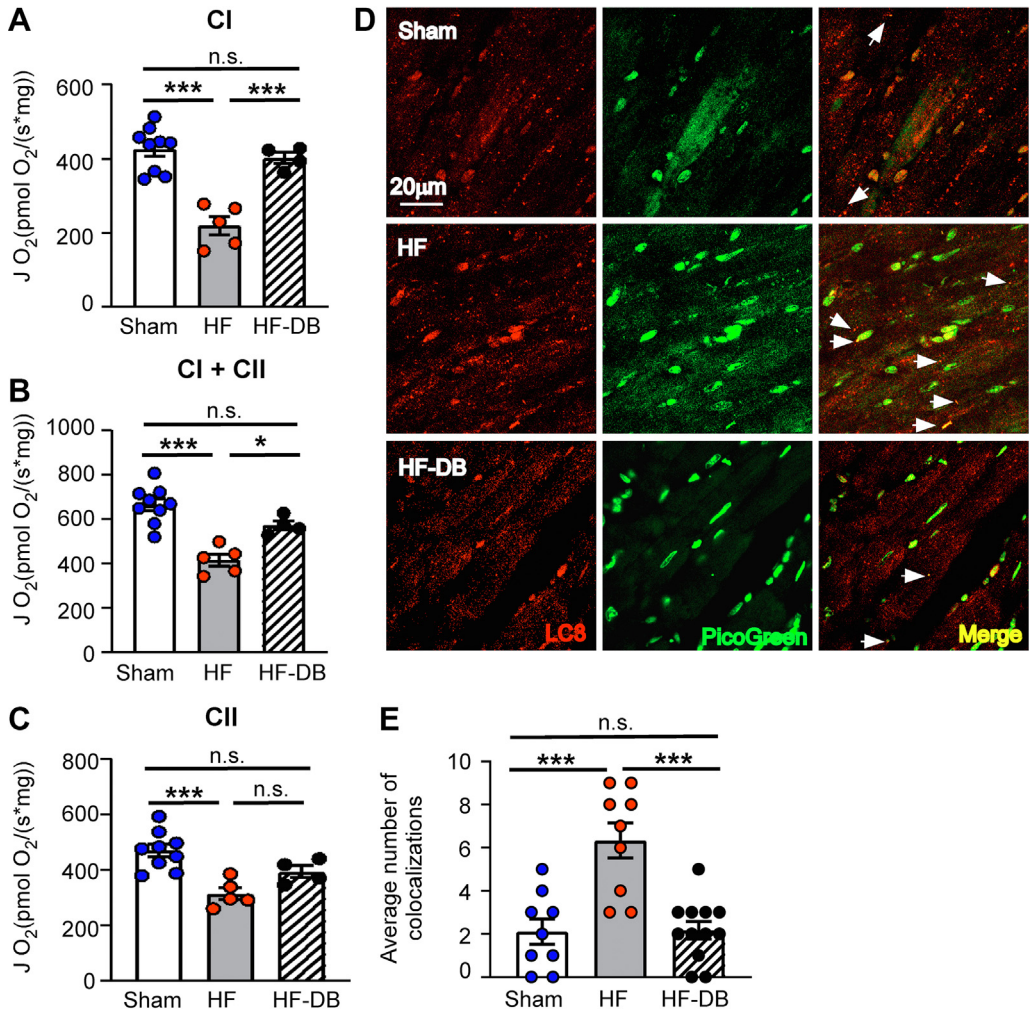

High-resolution respirometry was performed to measure oxygen consumption (JO2) in sham, HF, and HF-DB mice hearts (4-9 hearts/group) in the presence of **(A)** ADP (complex I) (Tukey test), **(B)** succinate (complex I + II) (Tukey test), and **(C)** rotenone (complex II) (Tukey test). **(D)** Representative fluorescent micrographs images of myocardial sections from sham, HF, and HF-DB mice depicting colocalization of PicoGreen **(green)** with an anti-LC3 antibody **(red)**. **White arrowheads** denote colocalization of PicoGreen and LC3 **(yellow fluorescence)**. Scale bar = 20 μm. **(E)** Group data for the number of yellow puncta reflecting the colocalization of PicoGreen and LC3 double-positive deposits (n = 9-12 fields from 3-4 mice /group) (Tukey test). *$P < 0.05$, ***$P < 0.001$. ADP = adenosine diphosphate; other abbreviations as in Figure 1.

observed in the heart.[13] Mice were treated with intravenous injections of AAV9-CMV-TFEB and AAV9-CMV-GFP (control) particles (at 3.5 X 10^{11} viral particles/mouse) and followed longitudinally for 4 weeks before terminal humane killing. Remarkably, there was 80% lethality in the AAV9-CMV-TFEB-treated HF mice (Figure 5A) relative to AAV9-CMV-GFP-treated HF mice, whereas there was no mortality in HF-DB mice treated with AAV9-CMV-TFEB or AAV9-CMV-GFP. Because the lethality occurred so rapidly after AAV9-CMV-TFEB treatment in the HF mice, we were not able to assess LV function.

FIGURE 5 Effect of TFEB-Mediated Enhancement of Autophagy in a Mouse Model of Reversible HF

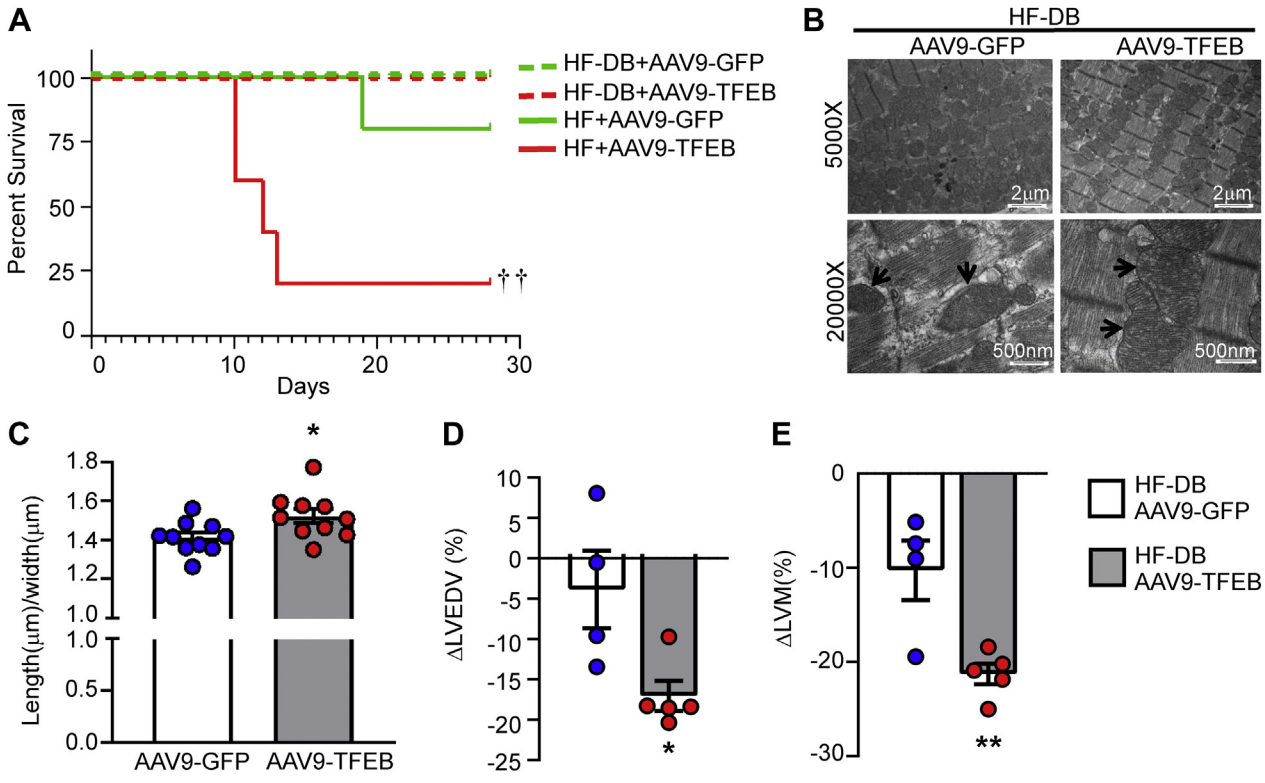

(A) Kaplan-Meier analysis of HF and HF-DB mice injected with adeno-associated virus 9 (AAV9)-cytomegalovirus (CMV)- transcription factor EB (TFEB) or AAV9-CMV-green fluorescent protein (GFP) (control). HF mice were injected 1 day after sham debanding surgery 2 weeks after transaortic constriction (TAC) + myocardial infarction (MI). HF-DB mice were injected 1 day after hemodynamic unloading (day 0) 2 weeks after TAC + MI (n = 5 mice/group/intervention) (log-rank). **(B)** Representative TEM images of myocardial sections of HF-DB mice injected with AAV9-CMV-TFEB or AAV9-CMV-GFP (6 weeks). **Black arrows** indicate mitochondria. Scale bars, 2 μmol/L **(upper)** and 500 nm **(lower)**. **(C)** Group data for mitochondrial aspect ratio (ratio length/width) in HF-DB mice treated with AAV9-CMV-TFEB or AAV9-CMV-GFP for 4 weeks (n = 9-12 images from 3-4 mice/group) (*t* test). Two-dimensional echocardiograms were performed 4 weeks after debanding in the AAV9 injected HF-DB mice and compared with the respective values at the time of debanding, before the injection of AAV9 (Supplemental Figure 1B). **(D)** Percent change in left ventricle (LV) end-diastolic volume in HF-DB mice treated with AAV9-CMV-TFEB or AAV9-CMV-GFP for 4 weeks (Mann-Whitney test). **(E)** Percent change in LV mass in HF-DB mice treated for 4 weeks with AAV9-CMV-TFEB or AAV9-CMV-GFP (n = 4-5 mice/group) (*t* test). *$P < 0.05$, **$P < 0.01$, ††$P < 0.01$ by log-rank. Abbreviations as in Figures 1 and 2.

Given the striking increase in mortality of AAV9-CMV-TFEB-treated HF mice in the setting of hemodynamic overload, we focused our studies on characterizing the effects of TFEB transduction in the HF-DB mice. Figure 5 indicates that AAV9-mediated TFEB transduction led to improved morphology of cardiac mitochondria in the HF-DB mice when compared with AAV9-CMV-GFP-treated HF-DB mice, as evidenced by the decreased rarefaction of the mitochondrial cristae (Figure 5B) and increased aspect ratio (Figure 5C) of the mitochondria ($P = 0.026$). The TFEB-mediated changes in mitochondrial morphology were accompanied by changes in LV structure. The salient finding shown by Figures 5D and 5E, respectively, is that AAV9-mediated TFEB transduction resulted in a decrease in LV end-diastolic volume ($P = 0.032$) and LV mass ($P = 0.009$) relative to AAV9-CMV-GFP-treated HF-DB control mice. There was, however, no difference in left ventricular ejection fraction (LVEF) in the HF-DB mice treated with AAV9-CMV-TFEB when compared with AAV9-CMV-GFP-treated mice ($P = 0.83$). Viewed together, these data suggest that enhancing the activation of TFEB leads to improved mitochondrial protein control and increased reverse LV remodeling in the HF-DB mice.

JACC: BASIC TO TRANSLATIONAL SCIENCE VOL. 7, NO. 12, 2022
DECEMBER 2022:1214–1228

DISCUSSION

Although the biological changes that are associated with reverse LV remodeling have been annotated by this and other laboratories (reviewed in Hellawell and Margulies[3], Mann et al [4], and Kim et al[23]), the precise biological mechanisms that allow the heart to revert toward a less pathologic phenotype and assume a more elliptical shape with a normal LV end-diastolic pressure-volume relationship are not known. We and others previously reported that reverse LV remodeling is associated with the emergence of new sets of myocardial genes that belong to ontogenies that are not expressed in nonfailing hearts,[5] including gene ontogenies involved in tissue repair.[6,7] Recognizing the emerging importance of protein quality control in a variety of diseases, including proteotoxic cardiomyopathy,[13,24] we sought to determine the role of the autophagy-lysosome pathway in a pathophysiologically relevant murine model of HF wherein hemodynamic unloading leads to reversal of the HF phenotype. Here we provide 3 new and important insights with respect to role of autophagy in reverse LV remodeling.

First, autophagic flux and mitochondrial respiration were impaired in the hearts of the HF mice (**Figures 1 and 4**) relative to sham-operated control mice. The decrease in flux resulted in an accumulation of damaged organelles, polyubiquitinated proteins, and more rounded mitochondria in the HF mouse hearts. Second, hemodynamic unloading of the HF-DB mice restored autophagic flux to levels observed in sham mice, and normalized mitochondrial oxidative respiration. Remarkably, we continued to observe damaged proteins and organelles in the HF-DB mouse hearts, despite normalization of autophagic flux, suggesting that flux was insufficient to restore cardiac myocyte proteostasis. Third, enhancing TFEB-mediated autophagic flux yielded disparate outcomes in the HF mice and the HF-DB mice. Whereas there was ~80% lethality in the HF mice ($P < 0.010$ compared with AAV9-CMV-GFP control mice) 10-14 days after AAV9-CMV-TFEB injection, AAV9-CMV-TFEB injection was safe in HF-DB mice and resulted in improved cardiac mitochondrial morphology, decreased LV end-diastolic volumes, and decreased LV mass (**Figure 5**), suggesting that enhancing autophagic flux led to more favorable reverse cardiac remodeling. The beneficial findings with respect to AAV9-CMV-TFEB injection in the HF-DB mice are consistent with a report by Sciarretta et al,[25] who demonstrated that treating mice with trehalose to enhance TFEB-mediated autophagy prevented the development of adverse LV remodeling and LV dysfunction in an acute coronary artery ligation model of chronic HF.

THE ROLE OF THE AUTOPHAGY-LYSOSOME PATHWAY IN CARDIAC REMODELING. Autophagy is an evolutionarily conserved intracellular mechanism that mediates degradation of large and long-lived proteins (including sarcomeres[26]), protein aggregates, entire defective organelles, as well as any cellular material that is too bulky for proteasomal degradation. The autophagy-lysosome system also serves as a dynamic recycling system that provides new building blocks for cellular renovation and homeostasis of cells.[27] Under normal physiological conditions, "basal" or constitutive autophagy is indispensable for cellular homeostasis, whereas under stressful conditions "adaptive autophagy" provides a short-term mechanism for cell survival.

Prior studies have established a critical role for basal autophagy in the heart.[28,29] Although the precise role of stress-induced adaptive autophagy in the heart is less well understood, the literature suggests that it is likely nuanced and context dependent. Shirakabe et al[30] reported that autophagic flux was increased from 1 to 12 hours after TAC, whereas flux was decreased several weeks after TAC, which is consistent with the findings presented herein, where we noted decreased autophagic flux in the hearts of HF mice 6 weeks after TAC + MI. Other studies have shown that markers of cardiac autophagy are increased after TAC in mice and remain elevated for several weeks. These findings were interpreted as suggesting that increased autophagy plays a role in the pathogenesis of hemodynamic overload-induced HF.[31] However, given that autophagic flux was not measured in this study, it is not clear whether the increased markers of autophagy were secondary to impaired flux or whether they were secondary to increased autophagy.

Increased autophagosomes and autophagic substrates (eg, p62 and ubiquitin) have also been reported in failing human hearts.[32,33] Whereas the accumulation of ubiquitinated proteins can be observed with impaired proteasome function, the accumulation of p62 and Lys63 ubiquitinated proteins are biological markers of insufficient autophagic clearance.[8,34] The failure to effectively restore essential cytosolic components (ie, insufficient autophagy) creates 2 biological problems that impact cellular resilience: first, the inability to replenish/restore properly functioning intracellular organelles and proteins (eg, sarcomeres) prevents cardiac myocytes from resuming normal contractile function; second, the accumulation of

damaged mitochondria/organelles and damaged proteins can lead to increased oxidative stress and increased endoplasmic reticulum stress response, respectively.[35,36] Moreover, increased levels of p62 can contribute to the persistent low-grade inflammation that has been observed in the failing heart,[37] insofar as p62 can promote the expression of inflammatory genes via nuclear factor kappa B.[38]

Although activation of autophagy has been shown to reduce chronic ischemic LV remodeling,[10,39,40] there is limited information with respect to the functional role of autophagy during the process of reverse LV remodeling. Autophagy is increased in wild-type hearts during regression of angiotensin II-induced cardiac hypertrophy after the removal of infusion mini-pumps,[41] and up-regulation of autophagy has been associated with increased reverse LV remodeling in mice after acute LAD ligation.[40,42] To date, only 2 experimental studies have examined autophagy after hemodynamic unloading in models of pressure overload-induced concentric LV hypertrophy.[43,44] Whereas 1 study in male rats subjected to 7-9 weeks of supravalvular aortic banding showed that autophagic flux was increased after aortic banding,[44] a study in mice reported opposite findings and showed that 1 week after TAC-induced hemodynamic overload autophagy markers were decreased, suggesting decreased autophagic flux.[43] Importantly, both studies demonstrated that autophagy was increased after hemodynamic unloading, consistent with the results presented herein. Relevant to this discussion, biopsy samples of LV myocardium from patients with idiopathic dilated cardiomyopathy at the time of implantation of a left ventricular assist device revealed that mechanical unloading of the failing human heart was associated with decreased markers of autophagy, suggesting that autophagy in the failing human heart is load dependent.[45] Further, increased autophagic vacuoles in cardiac myocytes (indicative of increased autophagy) was an independent predictor of reverse LV remodeling in hearts of patients with dilated cardiomyopathy who were treated with guideline- directed medical therapies.[46] This study also revealed that an increase in autolysosomes and expression of cathepsin D along with a reduction on autophagosome number correlated with reverse LV remodeling, suggesting a potential role for enhanced autophagic flux (as indicated by turnover to autophagosomes to form autolysosomes) in myocardial recovery.

Because of differences in experimental protocols and models, it is not clear from these studies whether the up-regulation of autophagy is necessary to repair damaged cardiac myocytes or whether it is instead deleterious. Our results suggests that the role of autophagy in the heart is dependent on the context in which it is studied. That is, we observed a striking increase in mortality in the HF mice treated with an AAV9-CMV-TFEB vector to enhance flux through the autophagy-lysosome pathway in the face of persistent hemodynamic overload; whereas the identical treatment at an identical time point had no effect on mortality and was associated with indices of improved reverse LV remodeling in the HF-DB mice with experimental reversal of TAC-induced hemodynamic overload. Although we cannot exclude the possibility that the increase in mortality in the AAV9-CMV-TFEB-treated HF mice was secondary to the toxic effects of sustained TFEB activation[47,48] or autosis,[49] the observation that sustained activation of TFEB was safe and beneficial in the HF-DB mice, as well as in mice with advanced proteotoxic cardiomyopathy,[13,24] suggests that the outcomes of enhancing autophagic flux will depend on the conditions in which flux is being studied.

Although the scope of the present study was not intended to precisely define the mechanistic pathways responsible for the regulation of autophagic flux in the HF and the HF-DB mice, the observation that mTOR activation was increased in the HF mice with impaired autophagic flux and that mTOR activation was decreased in HF-DB mice with restoration of autophagic flux in the HF-DB mice suggests (but does not prove) that mTOR activation state is one potential mechanism that regulates autophagic flux in the HF and HF-DB mouse hearts. A second limitation of the present study is that, although we demonstrate that enhancing autophagy through TFEB activation is sufficient to accelerate recovery of LV function and enhance reverse LV remodeling, the present study does not address the important question of whether autophagy is necessary for reverse LV remodeling. Accordingly, further studies will be required to evaluate whether macro-autophagy and mitophagy are essential for reverse LV remodeling after hemodynamic unloading. Lastly, insofar as the present studies were conducted in a murine model that mimics the combined effects of hypertension and ischemic heart disease, the results presented herein with respect to autophagy and reverse LV remodeling may not be applicable to all forms of HF with a reduced LVEF.

CONCLUSIONS

The results of this study demonstrate that reverse LV remodeling is associated with restoration of flux through the autophagy-lysosome pathway,

suggesting that autophagy may be an important biological mechanism that is required for restoring myocardial homeostasis after the resolution of tissue injury. The observation that restoration of flux was insufficient to completely remove damaged proteins and organelles in the HF-DB hearts may provide one explanation (albeit speculative) for why HF recurs (ie, relapse) in patients who have undergone reverse LV remodeling and improved their LVEF. The failure to effectively restore essential cytosolic components in cardiac myocytes leads to a loss of biological and contractile reserve capacity (ie, loss of "cellular resilience"[9]). Relevant to the present discussion, insufficient autophagy has been linked to worse clinical outcomes in patients with dilated cardiomyopathy,[32] increased fibrosis in idiopathic pulmonary fibrosis,[50] and persistent organ failure in critically ill sepsis patients.[51] Viewed together these observations raise the interesting possibility that enhancing the autophagy-lysosome pathway in cardiac myocytes can be leveraged clinically to provide a more durable recovery of LV structure and function (ie, sustained "remission"). Indeed, this pathway has become an area of intense interest in the biotechnology industry, which is developing therapeutics to enhance autophagy in neurodegenerative disease and aging.[52,53] However, our studies also strike a cautionary note with respect to the timing of therapeutic interventions that enhance autophagy in the failing heart, insofar as enhancing TFEB-mediated autophagic flux in HF mice was associated with increased lethality, whereas enhancing TFEB-mediated autophagic flux in HF-DB mice was safe and resulted in more favorable reverse LV remodeling. Accordingly, further preclinical studies will be required to address these interesting if not important questions.

FUNDING SUPPORT AND AUTHOR DISCLOSURES

This study was supported by research funds from the National Institutes of Health (R01HL147968, R01 HL155344), the Veterans Administration (AN # 4345132), and the Wilkinson Foundation to Dr Mann. Dr Diwan was supported by grants from the National Institutes of Health (HL107594, HL143431, and NS094692) and the Department of Veterans Affairs (I01BX004235). Dr Finck was supported by grants from the National Institutes of Health (R01 HL119225, P30 DK05634). Dr Kovacs was supported by grants from the National Institutes of Health (S10 OD028597). All other authors have reported that they have no relationships relevant to the contents of this paper to disclose.

ADDRESS FOR CORRESPONDENCE: Dr Douglas L. Mann, Cardiovascular Division, Washington University School of Medicine, 660 South Euclid Avenue, Box 8086, St. Louis, Missouri 63110, USA. E-mail: dmann@wustl.edu.

PERSPECTIVES

COMPETENCY IN MEDICAL KNOWLEDGE: Understanding the biological pathways that facilitate reverse LV remodeling in the failing heart is critical for targeting these pathways therapeutically. Our studies in a pathophysiologically relevant murine model of reversible HF show that, despite normalization of flux through the autophagy-lysosome pathway, restoration of flux was insufficient to completely remove damaged proteins and organelles in the cardiac myocytes. The failure to effectively restore essential cytosolic components in cardiac myocytes may lead to a loss of contractile reserve, which in turn may provide insights into the biological basis for why HF recurs (ie, relapse) in patients who have been treated with evidence-based medical and/or device therapies. Our studies further suggest that therapeutic targeting of the autophagy-lysosome pathway in HF may be possible in the future and may lead to improved LV reverse LV remodeling, but that the outcomes of this therapeutic approach are context dependent and will require additional preclinical studies to ensure the safety of this approach.

TRANSLATIONAL OUTLOOK: The basic mechanisms that allow the failing heart to recover after treatment with evidence-based medical therapies are not known. Here we demonstrate that hemodynamic unloading leads to normalization of LV structure and function that is accompanied by restoration of flux through the autophagy-lysosome pathway using a pathophysiologically relevant murine model of reversible HF. However, despite normalization of autophagic flux, there was incomplete removal of damaged proteins and organelles in cardiac myocytes, suggesting that restoration of flux is insufficient to completely restore myocardial proteostasis. Enhancing flux through the autophagy-lysosome pathway using AAV9-mediated gene therapy with TFEB in mice that underwent hemodynamic unloading resulted in more favorable reverse LV remodeling, whereas overexpressing TFEB in mice that have not undergone hemodynamic unloading resulted in increased mortality. These latter translationally oriented studies suggest that the role of autophagy in the heart is dependent on the context in which it is studied, and that further preclinical studies will be required to address the timing of interventions that enhance autophagic flux before this therapy can be advanced safely into clinical trials of patients with HF.

REFERENCES

1. Kass DA, Baughman KL, Pak PH, et al. Reverse remodeling from cardiomyoplasty in human heart failure. External constraint versus active assist. *Circulation*. 1995;91:2314–2318.

2. Levin HR, Oz MC, Chen JM, Packer M, Rose EA, Burkhoff D. Reversal of chronic ventricular dilation in patients with end-stage cardiomyopathy by prolonged mechanical unloading. *Circulation*. 1995;91:2717–2720.

3. Hellawell JL, Margulies KB. Myocardial reverse remodeling. *Cardiovasc Ther*. 2012;20:172–181.

4. Mann DL, Barger PM, Burkhoff D. Myocardial recovery: myth, magic or molecular target? *J Am Coll Cardiol*. 2012;60:2465–2472.

5. Margulies KB, Matiwala S, Cornejo C, Olsen H, Craven WA, Bednarik D. Mixed messages: transcription patterns in failing and recovering human myocardium. *Circ Res*. 2005;96:592–599.

6. Topkara VK, Chambers KT, Yang KC, et al. Functional significance of the discordance between transcriptional profile and left ventricular structure/function during reverse remodeling. *JCI Insight*. 2016;1 e86038:1–17.

7. Weinheimer CJ, Kovacs A, Evans S, Matkovich SJ, Barger PM, Mann DL. Load-dependent changes in left ventricular structure and function in a pathophysiologically relevant murine model of reversible heart failure. *Circ Heart Fail*. 2018;11:e004351.

8. Komatsu M, Waguri S, Koike M, et al. Homeostatic levels of p62 control cytoplasmic inclusion body formation in autophagy-deficient mice. *Cell*. 2007;131:1149–1163.

9. Smirnova L, Harris G, Leist M, Hartung T. Cellular resilience. *ALTEX*. 2015;32:247–260.

10. Ma X, Liu H, Foyil SR, et al. Impaired autophagosome clearance contributes to cardiomyocyte death in ischemia/reperfusion injury. *Circulation*. 2012;125:3170–3181.

11. Javaheri A, Bajpai G, Picataggi A, et al. TFEB activation in macrophages attenuates post-myocardial infarction ventricular dysfunction independently of ATG5-mediated autophagy. *JCI Insight*. 2019;4:e127312.

12. Evans S, Tzeng HP, Veis DJ, et al. TNF receptor-activated factor 2 mediates cardiac protection through noncanonical NF-kappaB signaling. *JCI Insight*. 2018;3:e98278.

13. Ma X, Mani K, Liu H, et al. Transcription factor EB activation rescues advanced alphaB-crystallin mutation-induced cardiomyopathy by normalizing desmin localization. *J Am Heart Assoc*. 2019;8:e010866.

14. Chambers KT, Cooper MA, Swearingen AR, et al. Myocardial Lipin 1 knockout in mice approximates cardiac effects of human LPIN1 mutations. *JCI Insight*. 2021;6:e134340.

15. Ma X, Rawnsley DR, Kovacs A, et al. TRAF2, an innate immune sensor, reciprocally regulates mitophagy and inflammation to maintain cardiac myocyte homeostasis. *J Am Coll Cardiol Basic Trans Science*. 2022;7:223–243.

16. Oka T, Hikoso S, Yamaguchi O, et al. Mitochondrial DNA that escapes from autophagy causes inflammation and heart failure. *Nature*. 2012;485:251–255.

17. Jimenez RE, Kubli DA, Gustafsson ÅB. Autophagy and mitophagy in the myocardium: therapeutic potential and concerns. *Br J Pharmacol*. 2014;171:1907–1916.

18. Li L, Wang ZV, Hill JA, Lin F. New autophagy reporter mice reveal dynamics of proximal tubular autophagy. *J Am Soc Nephrol*. 2014;25:305–315.

19. Ji CH, Kwon YT. Crosstalk and interplay between the ubiquitin-proteasome system and autophagy. *Mol Cells*. 2017;40:441–449.

20. Ueda H, Yamaguchi O, Taneike M, et al. Administration of a TLR9 inhibitor attenuates the development and progression of heart failure in mice. *J Am Coll Cardiol Basic Trans Science*. 2019;4:348–363.

21. Settembre C, Di Malta C, Polito VA, et al. TFEB links autophagy to lysosomal biogenesis. *Science*. 2011;332:1429–1433.

22. Godar RJ, Ma X, Liu H, et al. Repetitive stimulation of autophagy-lysosome machinery by intermittent fasting preconditions the myocardium to ischemia-reperfusion injury. *Autophagy*. 2015;11:1537–1560.

23. Kim GH, Uriel N, Burkhoff D. Reverse remodelling and myocardial recovery in heart failure. *Nat Rev Cardiol*. 2018;15:83–96.

24. Pan B, Zhang H, Cui T, Wang X. TFEB activation protects against cardiac proteotoxicity via increasing autophagic flux. *J Mol Cell Cardiol*. 2017;113:51–62.

25. Sciarretta S, Yee D, Nagarajan N, et al. Trehalose-induced activation of autophagy improves cardiac remodeling after myocardial infarction. *J Am Coll Cardiol*. 2018;71:1999–2010.

26. Masiero E, Agatea L, Mammucari C, et al. Autophagy is required to maintain muscle mass. *Cell Metabolism*. 2009;10:507–515.

27. Gerdes AM, Kellerman SE, Moore JA, et al. Structural remodeling of cardiac myocytes in patients with ischemic cardiomyopathy. *Circulation*. 1992;86:426–430.

28. Kuma A, Hatano M, Matsui M, et al. The role of autophagy during the early neonatal starvation period. *Nature*. 2004;432:1032–1036.

29. Nakai A, Yamaguchi O, Takeda T, et al. The role of autophagy in cardiomyocytes in the basal state and in response to hemodynamic stress. *Nat Med*. 2007;13:619–624.

30. Shirakabe A, Fritzky L, Saito T, et al. Evaluating mitochondrial autophagy in the mouse heart. *J Mol Cell Cardiol*. 2016;92:134–139.

31. Zhu H, Tannous P, Johnstone JL, et al. Cardiac autophagy is a maladaptive response to hemodynamic stress. *J Clin Invest*. 2007;117:1782–1793.

32. Saito T, Asai K, Sato S, et al. Autophagic vacuoles in cardiomyocytes of dilated cardiomyopathy with initially decompensated heart failure predict improved prognosis. *Autophagy*. 2016;12:579–587.

33. Hartupee J, Mann DL. Neurohormonal activation in heart failure with reduced ejection fraction. *Nat Rev Cardiol*. 2017;14:30–38.

34. Fujii S, Hara H, Araya J, et al. Insufficient autophagy promotes bronchial epithelial cell senescence in chronic obstructive pulmonary disease. *Oncoimmunology*. 2012;1:630–641.

35. Vanhorebeek I, Gunst J, Derde S, et al. Mitochondrial fusion, fission, and biogenesis in prolonged critically ill patients. *J Clin Endocrinol Metab*. 2012;97:E59–E64.

36. Gunst J, Derese I, Aertgeerts A, et al. Insufficient autophagy contributes to mitochondrial dysfunction, organ failure, and adverse outcome in an animal model of critical illness. *Crit Care Med*. 2013;41:182–194.

37. Torre-Amione G, Kapadia S, Lee J, et al. Tumor necrosis factor-a and tumor necrosis factor receptors in the failing human heart. *Circulation*. 1996;93:704–711.

38. Lee HM, Shin DM, Yuk JM, et al. Autophagy negatively regulates keratinocyte inflammatory responses via scaffolding protein p62/SQSTM1. *J Immunol*. 2011;186:1248–1258.

39. Erlebacher JA, Bhardwaj M, Suresh A, Leber GB, Goldweit RS. Beta-blocker treatment of idiopathic and ischemic dilated cardiomyopathy in patients with ejection fractions ≤20- percent. *Am J Cardiol*. 1993;71:1467–1469.

40. Kanamori H, Takemura G, Goto K, et al. Resveratrol reverses remodeling in hearts with large, old myocardial infarctions through enhanced autophagy-activating AMP kinase pathway. *Am J Pathol*. 2013;182:701–713.

41. Oyabu J, Yamaguchi O, Hikoso S, et al. Autophagy-mediated degradation is necessary for regression of cardiac hypertrophy during ventricular unloading. *Biochem Biophys Res Commun*. 2013;441:787–792.

42. Watanabe T, Takemura G, Kanamori H, et al. Restriction of food intake prevents postinfarction heart failure by enhancing autophagy in the surviving cardiomyocytes. *Am J Pathol*. 2014;184:1384–1394.

43. Hariharan N, Ikeda Y, Hong C, et al. Autophagy plays an essential role in mediating regression of hypertrophy during unloading of the heart. *PLoS One*. 2013;8:e51632.

44. Miranda-Silva D, Rodrigues GP, Alves E, et al. *Mitochondrial reversible changes determine diastolic function adaptations during myocardial (reverse) remodeling*. Circ Heart Fail; 2020: Circheartfailure119006170.

45. Kassiotis C, Ballal K, Wellnitz K, et al. Markers of autophagy are downregulated in failing human heart after mechanical unloading. *Circulation*. 2009;120:S191–S197.

46. Kanamori H, Yoshida A, Naruse G, et al. Impact of autophagy on prognosis of patients with dilated cardiomyopathy. *J Am Coll Cardiol*. 2022;79:789–801.

47. Du Bois P, Pablo Tortola C, Lodka D, et al. Angiotensin II induces skeletal muscle atrophy by activating TFEB-mediated MuRF1 expression. *Circ Res*. 2015;117:424–436.

48. Kenny HC, Weatherford ET, Collins GV, et al. Cardiac specific overexpression of transcription factor EB (TFEB) in normal hearts induces pathologic cardiac hypertrophy and lethal cardiomyopathy. *bioRxiv*. 2021:2021, 02.16.431474.

49. Nah J, Sung EA, Zhai P, Zablocki D, Sadoshima J. Tfeb-mediated transcriptional regulation of autophagy induces autosis during ischemia/reperfusion in the heart. *Cells*. 2022;11:258.

50. Araya J, Kojima J, Takasaka N, et al. Insufficient autophagy in idiopathic pulmonary fibrosis. *Am J Physiol Lung Cell Molec Physiol*. 2013;304:L56–L69.

51. Vanhorebeek I, Gunst J, Derde S, et al. Insufficient activation of autophagy allows cellular damage to accumulate in critically ill patients. *J Clin Endocrinol Metab*. 2011;96:E633–E645.

52. c&en. Cross R. Autophagy: drugging the yin and yang of the cell. 2019. https://cen.acs.org/business/start-ups/Autophagy-Drugging-yin-yang-cell/97/i22.

53. Rubinsztein DC, Codogno P, Levine B. Autophagy modulation as a potential therapeutic target for diverse diseases. *Nat Rev Drug Discov*. 2012;11:709–730.

KEY WORDS autophagy, reverse left ventricle remodeling

APPENDIX For supplemental figures, please see the online version of this paper.